Imaging of Endosome Fusion in BHK Fibroblasts Based on a Novel Fluorimetric Avidin-Biotin Binding Assay

Neil Emans, Joachim Biwersi, and A. S. Verkman
Departments of Medicine and Physiology, Cardiovascular Research Institute, University of California, San Francisco, CA 94143-0521 USA

ABSTRACT A fluorescence assay of in vivo endosome fusion was developed and applied to define the kinetics of endosome fusion in baby hamster kidney (BHK) fibroblasts. The assay is based on an ~10-fold enhancement of the green fluorescence of BODIPY-avidin upon biotin binding. The BODIPY-avidin fluorescence enhancement occurred in <25 ms, was pH-independent, and involved a BODIPY-tryptophan interaction. For endocytosis in vivo, BHK fibroblasts were pulse-labeled with BODIPY-avidin together with a red (rhodamine) fluorescent fusion-independent chromophore (TMR). After specified chase times in a nonfluorescent medium, a second cohort of endosomes was pulse-labeled with biotin-conjugated albumin, dextran, or transferrin. Fusion of biotin-containing endosomes with avidin-containing endosomes was quantified by ratio imaging of BODIPY-to-TMR fluorescence in individual endosomes, using imaging methods developed for endosome pH studies. Analysis of BODIPY-to-TMR ratio distributions in avidin-labeled endosomes exposed to zero and maximum biotin indicated >90% sensitivity for detection of endosome fusion. In avidin pulse (10 min) -chase-biotin albumin pulse (10 min) studies, both fused and unfused endosomes were identified; the fractions of avidin-labeled endosomes that fused with biotin-labeled endosomes were 0.48, 0.21, 0.16, and 0.07 for 0-, 5-, 10-, and 20-min chase times. Fitting of fusion data to a mathematical model of in vivo endosome fusion required the existence of an intermediate fusion compartment. Pulse-chase studies performed with biotin-transferrin to label the early/recycling endosomes indicated that after a 10-min chase, avidin-labeled endosomes reached a compartment that was inaccessible to biotin-transferrin. The assay was also applied to determine whether endosome fusion was influenced by temperature, pH (bafilomycin A1), second messengers (cAMP agonists, phorbol 12-myristate 13-acetate, staurosporine), and growth-related factors (platelet-derived growth factor, genistein). The results establish a sensitive fluorescence assay to quantify the fusion of vesicular compartments in living cells.

INTRODUCTION

Endocytic membrane traffic is a fundamental property of living cells that encompasses the sorting, recycling, and downregulation of internalized ligands and receptors, and the delivery of proteins to lysosomes for degradation (Goldstein et al., 1985; Gruenberg and Howell, 1989; Kornfeld and Mellman, 1989). Membrane fusion is a process that underlies the internalization of ligands/receptors from the plasma membrane and their delivery to early and then to recycling and/or late endosomal compartments. In addition, fusion of vesicles derived from the *trans*-Golgi allows the delivery of lysosomal enzymes to the endocytic pathway (Goda and Pfeffer, 1988, 1989, 1991).

Intact cell and cell-free assays have defined several populations of fusogenic endosomes in nonpolarized cells that are involved in the trafficking of internalized ligands (Gruenberg et al., 1989). Peripheral early endosomes are labeled by a brief incubation (1–5 min) with ligands destined to recycle to the plasma membrane (transferrin) and those destined to be transported to sorting/late endosomes (Salzman and Maxfield, 1988, 1989). Internalized fluid phase markers and lysosomally directed ligands are delivered to the perinuclear region with longer times of internalization (10–40 min) (Gruenberg et al., 1989). Much of the data used to construct this general scheme has come from pulse-chase experiments utilizing fluorescent and conventional biochemical markers to label various endosomal compartments (see Discussion); a real-time assay for study of endosome fusion in living cells has not been reported previously.

We describe here a sensitive fluorescence ratio imaging method to assay the fusion of endosomal vesicular compartments in living cells. Our strategy was to identify fluid-phase fluorophores that upon interaction generate a strong signal detectable by ratio imaging microscopy. Specific requirements for the components of the fusion assay were 1) lack of cytotoxicity, 2) cellular uptake by fluid-phase or receptor-mediated endocytosis, 3) essentially irreversible and pH-independent binding to one another, and 4) generation of a large fluorescence signal upon binding for ratio imaging. A suitable pair of compounds was identified after evaluating a number of candidate molecules, including fluorophore-quencher pairs and chromophore pairs that undergo fluorescence energy transfer (e.g., end-labeled oligonucleotides, fluorescein isothiocyanate (FITC)-avidin + rhodamine-biotin conjugates).

Our strategy to develop a fluorescence-based fusion assay was motivated by the reported small (1.3-fold) increase in FITC fluorescence in FITC-avidin upon binding of biotin (Przyjazny et al., 1993). After screening a series of fluoro-

Received for publication 23 February 1995 and in final form 24 April 1995.

Address reprint requests to Neil Emans, Ph.D., 1246 Health Sciences East Tower, Cardiovascular Research Institute, University of California, San Francisco, CA 94143-0521. Tel.: 415-476-8530; Fax: 415-665-3847; E-mail: emans@itsa.ucsf.edu.

0006-3495/95/08/716/13 $2.00

phore-conjugated avidins, it was found that the fluorescence of BODIPY-avidin increased strongly (~10-fold) upon binding of biotin. The photophysics of the fluorescence enhancement was studied by fluorescence lifetime and spectral measurements. For cell studies, the first component of the assay was BODIPY-avidin in which the reference (fusion-independent) chromophore tetramethylrhodamine was covalently linked to the avidin or added separately; the second component was biotin-albumin or biotin-dextran (to study fluid-phase endocytosis), or biotin-transferrin (to study early/recycling endosomes). [Avidin pulse]-[chase]-[biotin pulse] experiments were performed to determine the conditions under which internalized markers were directed by fusion events to a common endosomal compartment. Endosome fusion was assayed by quantitative ratio imaging of the fluorescence of individual endosomes, using hardware and software developed by our laboratory in a previous study of endosome pH (Zen et al., 1992). The new fusion assay was validated under cell-free conditions and in living cells and then applied to examine the kinetics of endosome fusion in BHK cells. The kinetic data were analyzed quantitatively, using a mathematical model of endosome fusion that incorporated concepts of endosome heterogeneity, an intermediate fusion compartment, and fusion inaccessibility. Effects of second messengers and other putative modulators of in vivo endosome fusion were then evaluated.

MATERIALS AND METHODS

Materials

Fluorescently-labeled avidins, amino dextran (10,000 mol wt), 5- and 6-carboxytetramethylrhodamine (TMR) succinimidyl ester, biotinamidocaproate-N-hydroxy succinimidyl ester, and rhodamine B dextran (40,000 mol wt) were purchased from Molecular Probes (Eugene, OR). Bovine serum albumin (BSA, serum free), biotinylated human transferrin, genistein, staurosporine, and bafilomycin A1 were obtained from Sigma Chemical Co. (St. Louis, MO), and phorbol 12-myristate-13-acetate (PMA) and platelet-derived growth factor from Boehringer Mannheim (Mannheim, Germany). Tissue culture reagents were obtained from the University of California-San Francisco Cell Culture Facility.

The fluid-phase markers amino dextran and BSA were biotinylated by reaction at 10 mg/ml in 0.1 M $NaHCO_3$ for 2 h at 20°C with a fivefold molar excess of biotinamidocaproate-N-hydroxy succinimidyl ester. Products were dialyzed against 10 mM Na_2CO_3 for 36–72 h and lyophilized. To synthesize BODIPY-TMR-avidin, BODIPY-avidin at 10 mg/ml in 0.1 M $NaHCO_3$ was reacted with a ninefold molar excess of TMR succinimidyl ester for 2 h at 20°C. The conjugate was dialyzed and lyophilized. A molar labeling ratio of 1:3.6:1 (TMR/BODIPY/avidin) was calculated, using molar extinction coefficients of 80,000 and 89,000 M^{-1} for TMR and BODIPY, respectively.

Cell culture and labeling procedures

Baby hamster kidney cells (BHK-21 (C-13) ATCC CCL 10, passages 1–15 after cloning) were cultured at 37°C in 95% air/5% CO_2 in DME-21 medium supplemented with 10% heat-inactivated fetal bovine serum (20 min at 56°C) and 1% penicillin-streptomycin. For experiments, cells were passed onto autoclaved 18-mm diameter round glass coverslips at a density of ~10^5 cells/ml and used when nearly confluent at 12–16 h after plating.

Before labeling, coverslips were washed three times in internalization medium (IM) (40 mM $NaHCO_3$, 75 mM NaCl, 5 mM KCl, 10 mM HEPES, 10 mM D-glucose, pH 7.4). The composition of this medium was optimized to reduce background fluorescence due to precipitation and/or binding of avidin to the cell surface. Cells were then incubated with fluorescent BODIPY-TMR-avidin (1 mg/ml) or BODIPY-avidin (1 mg/ml) + rhodamine B dextran (1 mg/ml) in IM at 37°C. After labeling, the coverslips were washed three times in IM. In some experiments, cells were then labeled with biotin-transferrin (180 μg/ml), biotin-dextran (2.4 mg/ml), or biotin-BSA (16 mg/ml) in serum-free, phenol red-free DME H21 at 37°C. Chases were performed in this medium. After labeling, cells were washed briefly in IM, mounted in a 200-μl perfusion chamber, in which the cell-free surface of the coverslip made contact with the immersion objective, and perfused with IM at 10–15°C.

Spectroscopic measurements

Steady-state fluorescence intensities were measured on an SLM 8000c fluorimeter (SLM Instruments, Urbana, IL) operating in the analog mode. Excitation/emission wavelengths (4-nm bandwidth) were 506/515 (BODIPY), 560/580 (TMR), and 280/330 (tryptophan). Kinetic measurements of BODIPY fluorescence enhancement were carried out on a Hi-Tech Sf51 stopped-flow apparatus equipped with excitation monochromator (495 nm) and emission cut-on filter (>515 nm); solution mixing and dead times were <2 ms (Van Hoek and Verkman, 1992). Time-resolved fluorescence was measured on an SLM 48000 Fourier transform multiharmonic fluorimeter using Ar laser (488 nm) excitation. Multi-frequency phase-modulation data were fitted to single or double lifetime decays (Thevenin et al., 1994).

Fluorescence microscopy

Cover glasses containing cultured cells were mounted in a perfusion chamber positioned on the stage of a noninverted epifluorescence microscope (Leitz) equipped with a Nipkow wheel confocal attachment (Technical Instruments, San Francisco, CA). Cells were illuminated by a stabilized Hg-Xe arc lamp using standard FITC (for BODIPY) and rhodamine (for TMR) filter sets. Fluorescence was collected by a 60× oil-immersion objective (Nikon Plan Apo, numerical aperture 1.4) and imaged by a 14-bit, 512× 512 pixel, cooled charged coupled device camera (AT200 series, Photometrics, Tucson, AZ) containing a high sensitivity back-thinned detector (TK512CB, Tektronix, Beaverton, OR). One linear micron mapped onto 4.4 pixels using the 60× objective in this optical system. Examination of the response linearity of individual pixel elements and flatfield/shading corrections were carried out, as described previously (Zen et al., 1992). Images were acquired using Photometrics PMIS software. A shutter was installed in the excitation path so that cells were illuminated only during image acquisition. In a typical experiment, the image was first manually focused using the rhodamine filter set. A TMR image was acquired over 2 s, the rhodamine filter set was exchanged for the FITC filter set (~2 s), and a BODIPY image was acquired over 2 s. Less than 2% photobleaching occurred under these conditions. Images were stored on a 230-MB magnetic hard disk and archived on 640-MB optical disks.

Image analysis

Quantitative ratio imaging of BODIPY-to-TMR fluorescence in individual endosomes was carried out using customized image processing software, as described by Zen et al. (1992). Well demarcated fluorescently labeled endosomes were identified in the rhodamine image; endosome area, generally 12–30 pixels, was defined on the basis of an algorithm utilizing maximum pixel intensity at the centroid of the endosome and background pixel intensity. Area-integrated pixel intensities of individual endosomes were then computed using as local background the median intensity in a single pixel layer surrounding each endosome. The same set of endosome areas was used to calculate area-integrated pixel intensities in the BODIPY

image. Because endosome x, y position in the TMR and BODIPY images was often slightly displaced (generally <2 pixels) because of wavelength-dependent focus and slow endosome movement, endosome boundaries defined in the TMR image were shifted individually in the BODIPY image to best overlay the recorded image. After area-integration and background subtraction in individual endosomes in the BODIPY image, BODIPY-to-TMR intensity ratios (B/T) were computed for each endosome. B/T ratios were relatively insensitive to the precise definition of endosome areas and boundary layers. Data were displayed as number versus B/T ratio histograms. The fraction of avidin-labeled endosomes that fused with biotin-labeled endosomes was estimated by linear regression of B/T histograms to a combination of distributions corresponding to unfused and 100% fused endosomes.

RESULTS

Cell-free experiments

The endosome fusion assay was based on the fluorescence enhancement of BODIPY-avidin upon binding of a biotinylated substrate. Fig. 1 *A* shows the effect of biotin on the fluorescence emission spectrum of BODIPY-tetramethylrhodamine avidin. There was a ~10-fold increase in BODIPY fluorescence with little change in TMR fluorescence. The fluorescence enhancement was very rapid, reaching 90% completion in under 25 ms, as assayed by stopped-flow fluorimetry (Fig. 1 *B*). The rapid response was not dependent on biotin concentration or pH (4–8), and the fluorescence signal enhancement of the BODIPY chromophore remained stable after biotin binding.

The influence of biotin on the fluorescence of a series of labeled avidins was tested. Biotin had little effect on the fluorescence of FITC- and TMR-avidin (Fig. 1 *C*) or on Texas Red- and Rhodol Green-avidin (enhancements of 1.2- and 2.1-fold, respectively; data not shown). In contrast, the fluorescence of BODIPY-avidin was strongly increased by ~10-fold by biotin. At high biotin concentration, the measured quantum yield of the BODIPY chromophore was 0.34. A slightly smaller maximum fluorescence enhancement was observed for BODIPY-tetramethylrhodamine avidin, as compared with that for BODIPY-avidin. Fluorescence increased linearly with biotin up to a biotin/avidin molar ratio of ~4, consistent with the presence of four biotin binding sites per avidin tetramer (Pugliese et al., 1993). Similar maximum fluorescence enhancements were

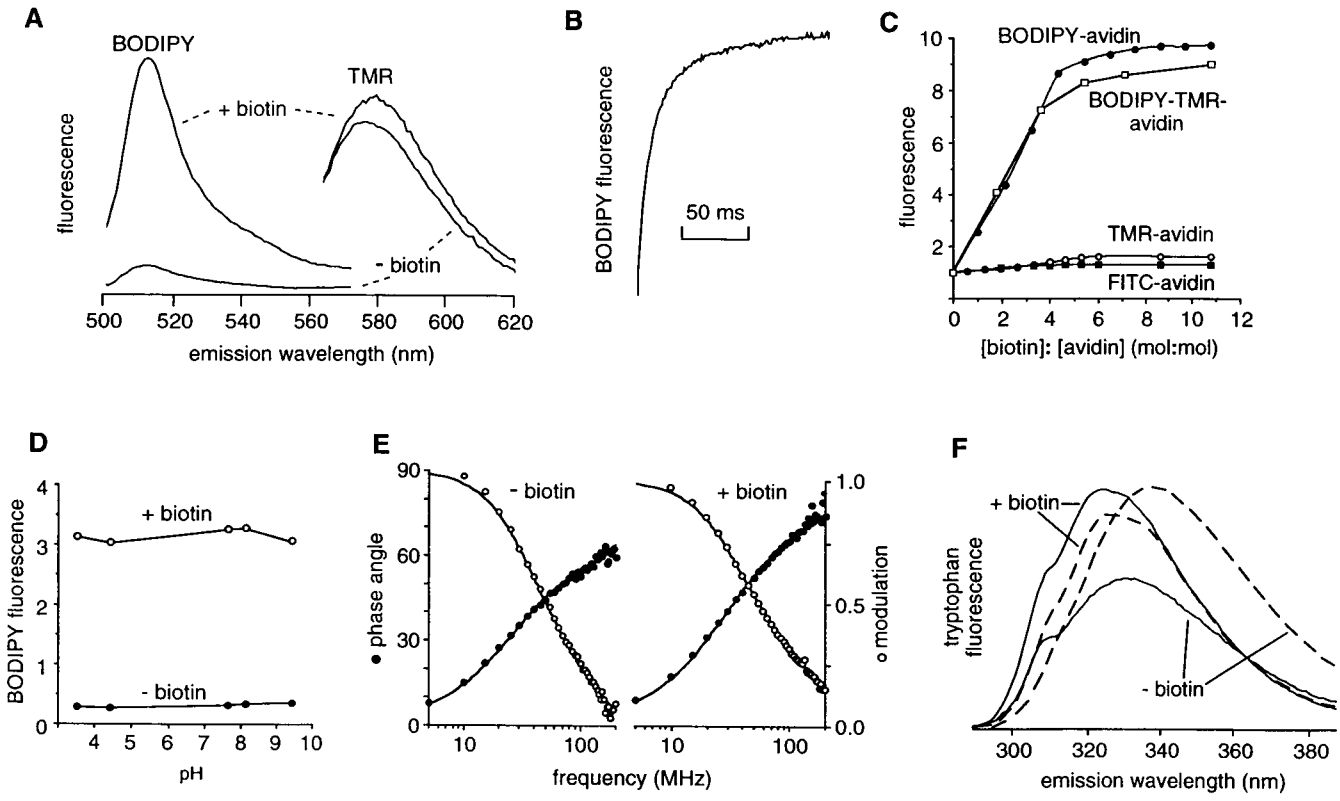

FIGURE 1 Solution characterization of the fluorescence enhancement of BODIPY-avidin upon binding of biotin. (*A*) Fluorescence emission spectrum of BODIPY-tetramethyl-rhodamine avidin (10 μg/ml) in IM buffer in the absence and presence of 1.5 mM biotin. Excitation wavelengths were 495 nm (BODIPY) and 555 nm (TMR). (*B*) Time course of BODIPY-avidin fluorescence (10 μg/ml) upon rapid (<1 ms) mixture with a 0.1 mg/ml solution of biotin-dextran in a stopped-flow apparatus. (*C*) Titration of the fluorescence enhancement of various fluorescently labeled avidins (each 10 μg/ml) with biotin at pH 7.4. (*D*) Dependence of BODIPY-avidin fluorescence on pH in IM buffer in the absence and presence of saturating concentrations of biotin. (*E*) Fluorescence lifetime analysis of BODIPY-avidin by phase-modulation fluorimetry. Phase angles and modulation ratios were fitted to a two-component fluorescence decay with lifetimes of 4.9 and 0.8 ns (−biotin) and 5.3 and 1.4 ns (+biotin). Fractional amplitudes of the shorter lifetime were 0.18 (−biotin) and 0.07 (+biotin). (*F*) Intrinsic tryptophan fluorescence of avidin (*dashed*) and BODIPY-avidin (*solid*) (both 200 nM) in the absence and presence of biotin. Excitation wavelength was 280 nm.

observed when biotin-dextran (10.6-fold), biotin-albumin (8.9-fold), and biotin-transferrin (8.4-fold) were used in place of biotin. Similar enhancements were also observed when pH was varied between 3.5 and 9.5. Fig. 1 *D* shows representative data for the fluorescence of BODIPY-avidin in the absence and presence of saturating concentrations of biotin. BODIPY fluorescence was insensitive to pH in the range 4.5–7.5 found in intracellular vesicular compartments.

To investigate the physical basis of the fluorescence enhancement of BODIPY-avidin upon biotin binding, BODIPY fluorescence lifetime analysis was carried out by phase-modulation fluorimetry (Fig. 1 *E*). The data fit well to a two-component decay model, with lifetimes and fractional amplitudes provided in the figure legend. The relatively small change in BODIPY lifetimes compared with the large fluorescence enhancement suggests that biotin binding induces a conformational change in the avidin molecule that alters BODIPY environment. To investigate the nature of the change in BODIPY environment that is responsible for the fluorescence enhancement, the intrinsic tryptophan fluorescence of BODIPY-avidin and unconjugated avidin was measured. Fig. 1 *F* shows that biotin binding is associated with a blue shift and an increase in tryptophan fluorescence of BODIPY-avidin (*solid lines*), resulting in a substantial shift in the emission maximum from 331 to 324 nm. In contrast, biotin binding caused a decrease in tryptophan fluorescence in the unconjugated avidin (*dashed lines*). Taken together with previous studies of BODIPY fluorescence properties and avidin structure (see Discussion), these results suggest that a biotin-dependent interaction between the tryptophan and BODIPY chromophores is responsible for the fluorescence enhancement.

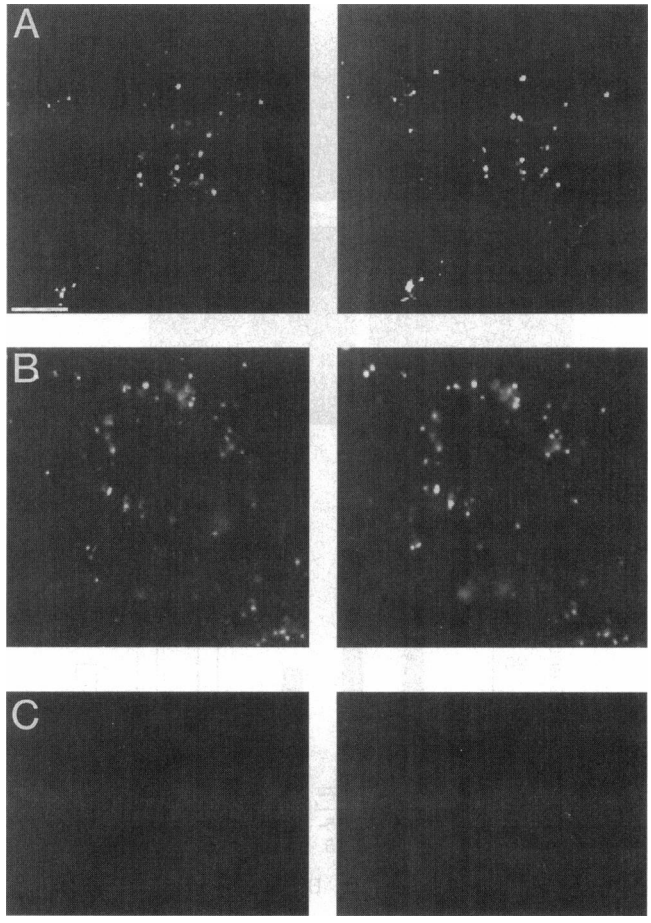

FIGURE 2 Photomicrographs of BODIPY-avidin uptake by BHK fibroblasts. Cells were pulse-labeled with BODIPY-avidin (1 mg/ml) and rhodamine B-dextran (1 mg/ml) for 10 min at 37°C (*A*), washed, and incubated at 37°C for 20 min (*B*). Images of BODIPY (*left*) and TMR (*right*) fluorescence are shown. Scale bar: 6 μm. (*C*) Same conditions except that the 10-min uptake was carried out at 4°C instead of 37°C.

Endocytosis in intact cells: control studies

Control experiments were performed next to show that BODIPY-conjugated avidin behaved as a fluid-phase marker in BHK fibroblasts under the conditions of our experiments. Cells were pulse-labeled with BODIPY-avidin (1 mg/ml) together with the fluid-phase marker rhodamine B-dextran (1 mg/ml) by incubation for 10 min at 37°C. The photomicrographs in Fig. 2 show colocalization of the BODIPY-avidin with rhodamine B-dextran at 10 min (*A*) and a 20 min (*B*) chase time after internalization. Note that over time the labeled vesicular compartments became brighter and localized in the perinuclear area. Quantitative analysis of endosome intensities indicated that the BODIPY-conjugated avidin colocalized with the rhodamine B-dextran over >30-min chase times. Fig. 2 *C* shows that low temperature blocked the internalization of BODIPY-avidin into distinct endosomes. These experiments indicate that fluorescently labeled avidin was internalized into vesicular compartments by fluid-phase endocytosis.

To characterize the sensitivity of the optical/imaging system for detection of a fusion signal in individual endosomes, the fluorescence of internalized BODIPY-avidin was quantified without and with maximum biotin binding. BHK fibroblasts were pulse-labeled for 10 min at 37°C with BODIPY-conjugated avidin in the absence or presence of biotin. Fig. 3 *A* shows the BODIPY and TMR fluorescence images. Qualitatively, biotin prebinding did not affect the TMR images, whereas endosomes in the BODIPY image were remarkably brighter. BODIPY-to-TMR fluorescence signal ratios (B/T) were computed from background-subtracted area-integrated pixel intensities, as described in Methods. Fig. 3 *B* shows a histogram of percentage endosomes versus B/T ratio. For graphical presentation, geometrically increasing B/T ratio intervals (0.25, 0.5, 1.0, etc.) were utilized, recognizing that any consistent choice of intervals would be valid. There was good separation of peaks corresponding to endosomes labeled with BODIPY-avidin in the absence (*filled bars*) and presence (*open bars*) of biotin. A threshold value of B/T = 1.9 established in >90% of endosomes whether or not biotin prebinding had occurred. To demonstrate that endosomal pH did not affect

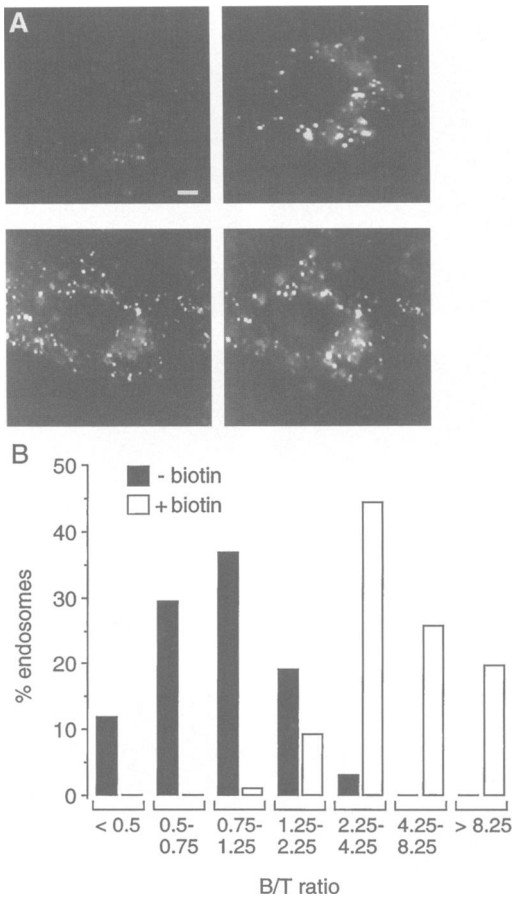

FIGURE 3 Internalization of BODIPY-avidin without and with prebinding of biotin. (*A*) BHK fibroblasts were labeled for 10 min with BODIPY-avidin (1 mg/ml) at 37°C in the absence (*top*) and presence (*bottom*) of biotin (1.5 mM). Photomicrographs were obtained of BODIPY (*left*) and TMR (*right*) fluorescence. Illumination, imaging, and display conditions were identical for all micrographs. Scale bar: 3 μm. (*B*) Histogram of number versus BODIPY-to-TMR fluorescence signal ratio. Data are shown for 165 endosomes from 20 different cells.

B/T signal ratios, images of BODIPY-avidin labeled endosomes were acquired after a 10-min chase in which the average endosome pH was <6 (Zen et al., 1992) and then 5 min after perfusion with 20 mM NH_4Cl, a weak base that alkalinized pH to ~7.5. The ratio of B/T before versus after NH_4Cl infusion was 1.06 ± 0.1 (SE, n = 30 endosomes). It is noted that under ideal conditions, a single value for the B/T signal ratio should be measured in every avidin-labeled endosome in the absence of biotin and a single ratio at maximum biotin. The finite width of the percentage versus B/T ratio histograms represents measurement uncertainties, including electronic noise in the detection of low light level images, and limitations in image analysis of the small fluorescent vesicles (Shi et al., 1991; Zen et al., 1992; see Discussion).

Kinetics of endosome fusion in intact cells

After the ability to detect the BODIPY fluorescence enhancement in biotin-containing endosomes was established, the kinetics of endosome fusion in BHK fibroblasts was investigated. Cells were labeled with the fluorescent avidin for 10 min at 37°C, chased with nonfluorescent medium at 37°C for 0 or 10 min, and then labeled for 10 min with biotin-albumin. The ability of the cohort of biotin-labeled endosomes to catch up and fuse with the avidin-labeled endosomes was quantified. Fig. 4 *A* shows representative BODIPY (*left*) and TMR (*right*) images of BHK fibroblasts chased for 0 min (*top*) and 10 min (*bottom*) with nonfluorescent medium. Qualitatively, a greater fraction of endosomes in the nonchased cells have bright BODIPY fluorescence. B/T signal ratios for eight endosomes in each condition are given in the figure legend. Fig. 4 *B* shows a histogram of percentage versus B/T ratio for 15 separate sets of experiments, including the analysis of ~2500 individual endosomes; histograms obtained from individual experiments (performed on ~10 cells during the same day) were similar in shape and position to the composite histogram in Fig. 4 *B*. Compared with the histogram in Fig. 3 *B*, the distributions from cells exposed to biotin-albumin are wider (*open and hatched bars*), indicating the presence of both fused and unfused avidin-containing endosomes. As the chase time between the avidin and biotin pulses was increased from 0 to 10 min, the fraction of fused endosomes decreased. Regression analysis of histograms indicated that the fraction of fused endosomes (f_{fusion}) at 0-, 5-, 10-, and 20-min chase times was 0.48, 0.21, 0.16, and 0.07, respectively. A summary of all experiments performed is provided in Table 1.

The determination of f_{fusion} by regression analysis of percentage versus B/T ratio histograms is based on the assumption that the finite width of the histogram is due to a combination of measurement signal noise (see Fig. 3 *B*) and the presence of two distinct endosome populations: fused and unfused endosomes. Additional broadening of the width of the histogram would result from partial states of fusion in which the B/T signal ratio (if measured without signal noise) was between 1 (minimum ratio, unfused) and the maximum ratio corresponding to complete fusion. Intermediate values of B/T would occur if some but not all avidin molecules in a single endosome bound biotin (see Fig. 1 *C*). To assure an all-or-none fusion signal, the experiments in Fig. 4 *B* were carried out using a large molar excess of biotin conjugate (16 mol per mol avidin). To examine whether the fusion signal was dependent on biotin concentration, experiments were carried out using two- and four-fold lower concentrations (8 and 4 mol per mol avidin). Similar histograms were found for a 10-min avidin pulse/10-min biotin pulse study carried out with internalized biotin-to-avidin molar ratios of 16 and 8, and a small left shift at a molar ratio of 4. Regression analysis gave f_{fusion} values of 0.52, 0.49, and 0.35 for molar ratios of 16, 8, and 4, respectively, supporting the conclusion that few endosomes had a partial fusion signal. Another concern in the quantitative analysis of fusion data was that results were biased because some endosomes were brighter than others. To minimize bias, endosomes were computer-selected in

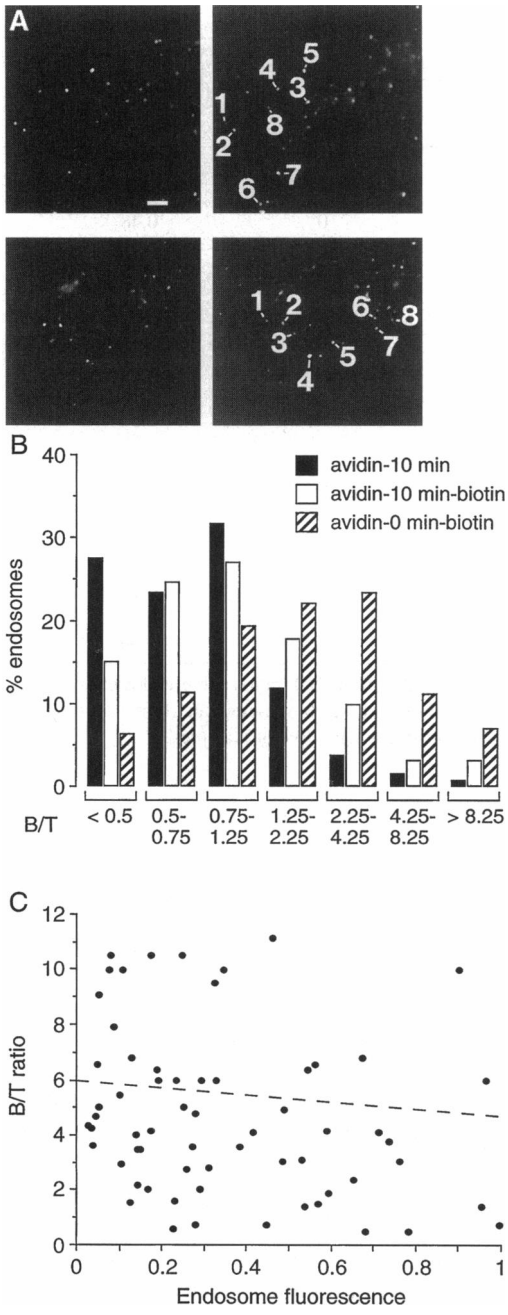

FIGURE 4 Effect of chase time on fusion of biotin-labeled endosomes with a cohort of avidin-labeled endosomes. Endosomes were labeled with BODIPY-avidin (1 mg/ml) for 10 min at 37°C, chased for 0 or 10 min with marker-free medium, and labeled for 10 min with biotin-albumin (16 mg/ml). (*A*) Micrographs of BODIPY (*left*) and TMR (*right*) images corresponding to the 0-min (*top*) and 10-min (*bottom*) chase times. Eight randomly chosen endosomes in each TMR image have been selected as indicated. B/T ratio values for the 0-min chase were 1) 3.4, 2) 3.2, 3) 3.9, 4) 2.8, 5) 1.9, 6) 3.0, 7) 2.6, and 8) 2.9. B/T ratio values for the 10-min chase were 1) 4.1, 2) 2.0, 3) 0.6, 4) 3.4, 5) 3.2, 6) 0.7, 7) 2.5, and 8) 0.5. Scale bar: 3 μm. (*B*) Histograms of number versus B/T ratio for avidin-labeled endosomes not exposed to biotin (*solid bars*) and exposed to biotin-albumin for 10 min after a 10-min chase (*open bars*) or 0-min chase (*hatched bars*) in marker-free medium. The analysis was carried out on 2478 endosomes in 15 independent sets of experiments. See text for details and Table 1 for fitted results. (*C*) Relationship between B/T signal ratio and endosome-integrated rhodamine signal intensity for a representative 10-min avidin pulse/10-min biotin pulse experiment.

the rhodamine (fusion-independent) image using an algorithm that detected bright and relatively dim endosomes with equal probability (Zen et al., 1992). Two analyses were carried out to investigate brightness-dependent bias in the data analysis. First, little correlation was found between B/T signal ratio and integrated endosome intensity (in the rhodamine channel) (Fig. 4 *C*) under conditions in which the fusion fraction was ~0.5. Second, it was found that the averaged B/T signal ratio differed from the intensity-weighted averaged B/T signal ratio by <5%; for example, unweighted and intensity-weighted averaged B/T signal ratios for the data in Fig. 4 *B* were 2.90 and 2.86, respectively.

Pulse-chase experiments were next carried out in which biotin-albumin, a fluid-phase marker, was replaced by biotin-transferrin, a marker of the early/recycling endosomal compartment. Control studies indicated that 500 μg/ml biotin-transferrin effectively blocked endosome labeling by 100 μg/ml FITC-transferrin. Fig. 5 *A* shows that a significant fraction (f_{fusion} = 0.43) of the avidin-labeled endosomes displayed a fusion signal at 0-min chase; however, essentially no endosomes (fitted f_{fusion} = 0) were fused after a 10-min chase, as indicated by the nearly identical histograms for the avidin alone (*filled bars*) and [avidin pulse]-[10-min chase]-[transferrin biotin pulse] (*open bars*) data. These results indicate that after 10 min, avidin-labeled endosomes enter a compartment that is inaccessible to internalized transferrin.

The effects of a series of putative modulators of endosome fusion were evaluated (Fig. 5, *B–F*; see Table 1 for summary). Second messenger modulation of protein kinase A and C pathways was first studied. It has been proposed that cAMP agonists decrease the rate of internalization of fluid-phase markers by causing a generalized decrease in endosome fusion (Bradbury et al., 1992). Fig. 5 *B* shows the effect of the cAMP agonist forskolin on endosome fusion. BHK cells were labeled with fluorescent avidin for 10 min, chased for 10 min in nonfluorescent medium, and then labeled for 10 min with biotin-albumin as in Fig. 4 *B*. Forskolin was present continuously from 15 min before avidin internalization and throughout the experiment. Consistent with previous data (Bradbury et al., 1992; Zen et al., 1992), forskolin decreased the number of endosomes noticeably by ~50%. However, as seen in Fig. 5 *B*, forskolin had no significant effect on endosome fusion. The fitted value of f_{fusion} was 0.16 in control and 0.18 in the presence of forskolin. These results suggest that forskolin inhibition of endocytosis is not related to inhibition of endosome fusion. Activation of protein kinase C by phorbol esters and protein kinase inhibition by the relatively nonspecific compound staurosporine affect various processes involved in endocytic uptake and endosome transport (Constantinescu et al., 1991; Fallon and Danaher, 1992). Fig. 5 *C* shows that in BHK fibroblasts, PMA caused slight inhibition of endosome fusion. It was shown previously that PMA addition under these conditions produces a rapid acidification of early endosomes (Zen et al., 1992). Staurosporine caused significant inhibition of endosome fusion, observed as the

TABLE 1 Summary of endosome fusion experiments

	Maneuver					
	Avidin (min)	Chase (min)	Biotin (min)	Chase (min)	f_{fusion}	n
Pulse chase: biotin-BSA						
	10	10	0	0	0.00	913
	10	0	10	0	0.48	1198
	10	5	10	0	0.21	278
	10	5	10	10	0.29	65
	10	10	10	0	0.16	367
	10	20	10	0	0.07	136
Pulse chase: biotin-Tf						
	10	0	10	0	0.43	77
	10	10	10	0	0.00	63
Effectors						
Bafilomycin A1 (1 μM)	10	0	10	0	0.31	164
Genistein (4 μM)	10	0	10	0	0.21	252
PMA (100 nM)	10	0	10	0	0.27	195
PDGF (100 ng/ml)	10	0	10	0	0.25	130
Staurosporine (2 μM)	10	0	10	0	0.14	116
Forskolin* (50 μM)	10	10	10	0	0.18	111
24°C‡	10	10	10	0	0.00	103

Incubations were performed at 37°C unless otherwise indicated. The value of f_{fusion} was calculated from B/T ratios for n endosomes, as described in Methods. Experiments were performed with the specified times for BT-avidin (1 mg/ml) pulse, chase, biotin-albumin (biotin-BSA: 16 mg/ml) or biotin-transferrin (biotin-Tf 180 μg/ml) pulse, and final chase. Underlined incubation time indicates where effector was present.

*15-min preincubation at 37°C with effector was performed before labeling.

‡Entire experiment performed at 24°C.

left shift in the B/T distribution (Fig. 4 *C*) and the decreased fitted f_{fusion} value (Table 1). There was no significant effect of staurosporine on endocytic uptake in these experiments based on the uptake of FITC-dextran. These results are consistent with the observation that cell-free fusion of early endosomes may be regulated by a protein kinase (Woodman et al., 1992).

Temperature is known to affect several steps in vesicular transport. Endocytosis in BHK fibroblasts is arrested at 4°C and was found to be slowed by ~80% at 23°C compared with 37°C. To study temperature effects on endosome fusion, all steps in the avidin pulse-chase-biotin albumin pulse experiments were carried out at 23°C and not at 37°C (Fig. 5 *D*). There was no apparent endosome fusion at 23°C, with a fitted f_{fusion} value of zero.

Several recent lines of evidence suggest that inhibition of endosomal acidification by bafilomycin A1 affects various steps in endosome and secretory vesicle transport, including the transport of fluid-phase markers from early to late endosomes (Clague et al., 1994), virus internalization and budding (Palokangas et al., 1994), and *trans*-Golgi network recycling (Reaves and Banting, 1994). The effect of bafilomycin A1 on endosome fusion was investigated using a [10-min avidin pulse]-[10-min biotin-albumin pulse] protocol (Fig. 5 *E*). Under the conditions of this study, bafilomycin A1 blocks the vacuolar proton pump and causes rapid alkalinization of the *trans*-Golgi (Seksek et al., 1995) and endosomal compartments (measured as described in Zen et al., 1992, data not shown). It was found that bafilomycin A1 caused a minor inhibition of endosome fusion (Fig. 5 *E*), decreasing f_{fusion} from 0.48 to 0.31. Based on cell-free fusion studies showing that bafilomycin A1 does not inhibit fusion of early endosomes (Clague et al., 1994), our finding suggests that the bafilomycin A1-sensitive component of fusion involves fusion of biotin-labeled endosomes with a post-early avidin-labeled compartment.

It was demonstrated recently that various growth factor-related ligands modulate endocytosis and that the tyrosine kinase inhibitor genistein slows internalization of various ligands (Luton et al., 1994; Fallon et al., 1994; Pure and Tardelli, 1992). There was significant inhibition of endosome fusion by genistein (Fig. 5 *F*) and a similar effect of platelet-derived growth factor (Table 1). Additional studies are required to define mechanistically the site(s) of action of these agents.

Mathematical model of endosome fusion

The experimental data above provide information about the kinetics of endosome fusion in BHK fibroblasts and on the influence of putative effectors of endosome fusion (Figs. 4 and 5). The fitted parameter describing each experimental condition is f_{fusion}, the fraction of avidin-labeled endosomes that fused with biotin-labeled endosomes. Several distinct cellular factors can influence endosome fusion, i.e., the ability of endosomes in the second biotin-labeled cohort to catch up and fuse with avidin-labeled endosomes in the first cohort. These factors include heterogeneity in endosome transport rates, the characteristics of intermediate compart-

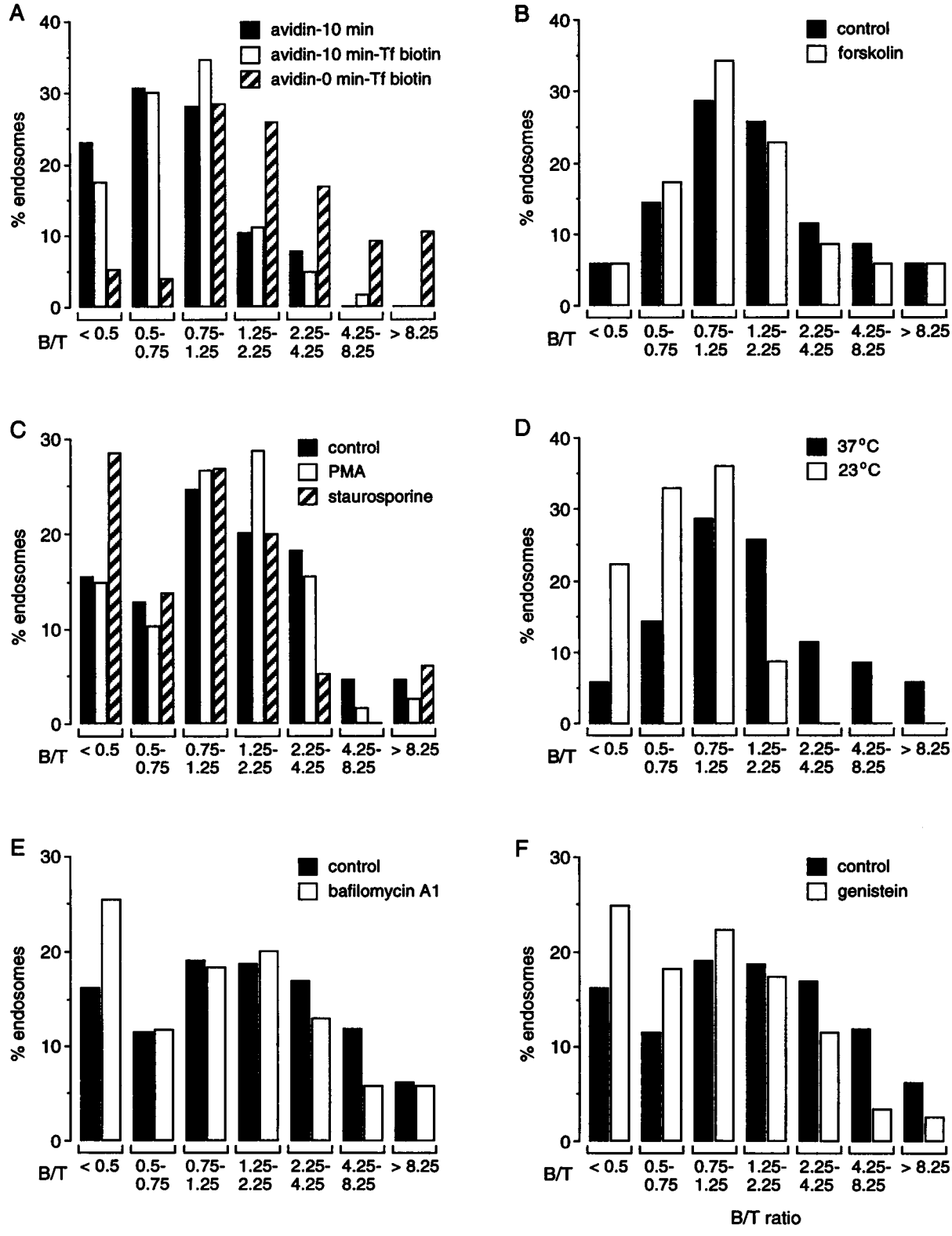

FIGURE 5 B/T ratio distributions for fusion of avidin-labeled endosomes with early/recycling endosomes (*A*) and influence of putative effectors on endosome fusion (*B–F*). See Table 1 for numbers of endosomes analyzed and fitted f_{fusion} values. (*A*) Endosomes were labeled as in Fig. 4 *B*, except that biotin-albumin was replaced by biotin-transferrin. (*B*) Endosomes were labeled with fluorescent avidin, chased for 10 min, and then labeled with biotin-albumin. Forskolin (50 μM) was present at 15 min before and throughout the experiment. (*C*) Effects of PMA (100 nM) and staurosporine (2 μM) studied in cells labeled with fluorescent avidin and then with biotin-albumin without chase period. (*D*) Experiment as in Fig. 4 *B* (10-min chase) was carried out entirely at 23°C or 37°C. (*E* and *F*) Effects of bafilomycin A1 (1 μM) and genistein (4 μM) on endosome fusion utilizing the [avidin pulse]-[biotin-albumin] pulse protocol.

ments in which endosome transport is transiently slowed, and the existence of fusion-inaccessible compartments in which endosome fusion cannot occur. These canonical factors incorporate various cellular factors, such as distinct endosome compartments (early, recycling, sorting, and late), endosome transport along cytoskeletal structures, and the modulation of activities and distributions of fusion-promoting factors.

Despite the potential complexity of these cellular factors, it is constructive to analyze the experimentally determined f_{fusion} values quantitatively by use of a mathematical model of in vivo endosome fusion. The model described in the Appendix predicts f_{fusion} based on the actual experimental pulse-chase times, incorporating the possibilities of endosome heterogeneity, an intermediate compartment, and a fusion-inaccessible compartment. Briefly, avidin- and biotin-labeled endosomes are generated at randomly chosen times during the respective pulse periods. Endosome heterogeneity is introduced (if desired) by ascribing a Gaussian distribution to endosome transport rates. An intermediate compartment (IC), defined by location and an exponentially distributed mean residence time, represents a short time in which endosome transport is arrested yet able to undergo fusion events. Finally, a fusion-inaccessible compartment, in which endosome fusion cannot occur, can be introduced by specifying a location parameter. The model predicts f_{fusion} and localizes the site of fusion with respect to the IC as early fusion (proximal to the IC), fusion in the IC, or late fusion (distal to the IC). The key feature of the model is that very few adjustable parameters are required to fit data and to generate experimental predictions: there is one parameter for endosome heterogeneity, two parameters for the IC, and one parameter for fusion inaccessibility.

The model was first used to fit f_{fusion} values for pulse-chase studies ([10-min avidin pulse]-[chase]-[10-min biotin-albumin pulse]) in which the chase time was varied between 0 and 20 min (see Table 1). Fig. 6 *A* shows the experimentally derived f_{fusion} values (*filled circles*) together with best fitted model predictions; model parameters are given in the figure legend. The principal conclusion was that models incorporating endosome heterogeneity were unable to provide an adequate fit to the data. Inclusion of an intermediate compartment with 15-min mean residence time and distance parameter 2 (without endosome heterogeneity or a fusion inaccessible compartment) yielded a good fit to the data. Utilizing the same fitted parameters, the [avidin pulse]-[5-min chase]-[biotin pulse]-[10-min chase] experiment was modeled. The model predicted that inclusion of the final 10-min chase increased f_{fusion} by 0.073, similar to that of 0.08 measured experimentally (rows 3 and 4, Table 1).

Additional model predictions and sensitivities are explored in Fig. 6, *B* and *C*. Fig. 6 *B* shows the dependence of f_{fusion} on the two parameters describing the intermediate compartment: the mean residence time and the distance to the compartment. f_{fusion} increased strongly with increasing mean residence time, and was less sensitive to the distance

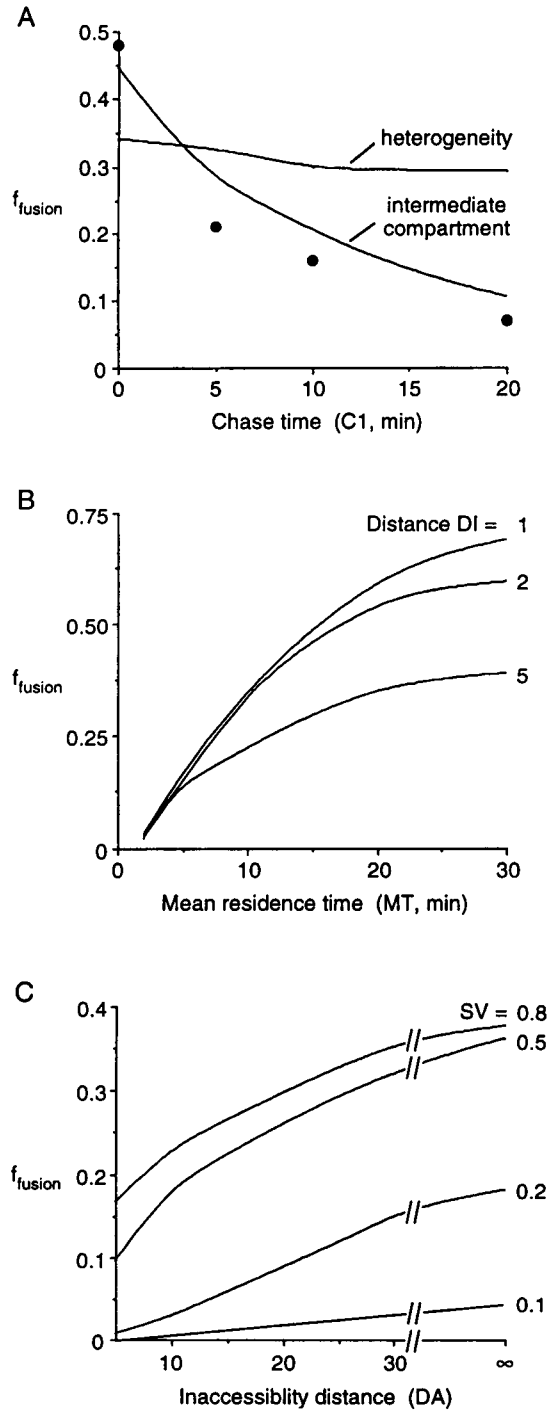

FIGURE 6 Predictions of the mathematical model for in vivo endosome fusion. Computations were performed as described in the Appendix. (*A*) Fitting of data for the dependence of the fraction of avidin-labeled endosomes that fused with biotin-labeled endosomes (f_{fusion}) as a function of chase time in [10-min avidin pulse]-[chase]-[10-min biotin-albumin pulse] studies. Experimental results shown as filled circles. Fitted curve labeled intermediate compartment calculated with $SV = 0$, $DA = 10^6$, $DI = 2$, $TM = 15$. Curve-labeled heterogeneity calculated with $SV = 2$, $DA = 10^6$, $TM = 0$. (*B*) Dependence of f_{fusion} on mean residence time in intermediate compartment (*TM*) and distance to intermediate compartment (*DI*) in a [10-min avidin pulse]-[10-min biotin-albumin pulse] protocol with $SV = 0$, $DA = 10^6$. (*C*) Dependence of f_{fusion} on heterogeneity in endosome velocity (*SV*) and fusion inaccessibility distance (*DA*) in a [10-min avidin pulse]-[10-min biotin-albumin pulse]-[30-min chase] protocol with $TM = 0$.

parameter. It is therefore predicted that the transit time through multivesicular bodies and similar sorting compartments in cells should strongly influence endosome fusion. In the absence of an intermediate compartment, Fig. 6 *C* shows the dependence of f_{fusion} on heterogeneity in endosome velocity and the distance to a fusion-inaccessible compartment. In the absence of a fusion-inaccessible compartment, increased endosome heterogeneity promotes fusion because faster biotin-labeled endosomes can catch up and fuse with avidin-labeled endosomes. Fusion is strongly inhibited by inclusion of a fusion-inaccessible compartment. The loss of fusion observed for the 10-min chase time in the biotin-transferrin study (see Table 1) is modeled in this way: avidin-labeled endosomes enter a fusion-inaccessible compartment from which biotin-transferrin-labeled endosomes are excluded.

DISCUSSION

The principal goal of this study was to establish a sensitive, spatially resolved fluorescence assay of endosome fusion in living cells. The assay exploited the large enhancement in the fluorescence of BODIPY-conjugated avidin upon biotin binding. The assay components had the required characteristics specified in the introduction, including lack of cytotoxicity, irreversible and pH-independent fluorescence enhancement, and when a second chromophore (TMR) was present, generation of a large fluorescence signal suitable for quantitative ratio imaging microscopy. The BODIPY-conjugated avidin functioned as a fluid-phase marker of endocytosis in BHK fibroblasts under the conditions of our experiments, as demonstrated by colocalization with rhodamine-dextran. The suitability of BODIPY-conjugated avidin as a fluid-phase marker should be confirmed for application of this fusion assay in different cell systems or for longer internalization times. As discussed below, pulse-chase studies defined the basic kinetic properties of endosome fusion in BHK fibroblasts and examined empirically the influence of putative modulators of in vivo endosome fusion.

The application of a fluorescence-based avidin-biotin assay to quantify endosome fusion in living cells is supported by a considerable body of data from cell-free endosome fusion studies that exploit the binding of avidin to biotinylated conjugates (Braell, 1992; Gorvel et al., 1991; Gruenberg et al., 1989). Technically, endosomal populations from different groups of cells are labeled separately with avidin and biotin markers, endosomes are isolated, and fusion is quantified by conventional biochemical methods such as immunoprecipitated enzyme activities (Braell, 1992; Gruenberg and Gorvel, 1992). Avidin and biotin markers have been utilized because their binding is essentially irreversible (K_d, 10^{-15} M; Green, 1963) and insensitive to pH, ionic strength, and temperature (Green, 1975); in addition, the ability to conjugate biotin with fluid-phase markers (Braell, 1992; Gruenberg and Gorvel, 1992) and receptor-associated markers permits the labeling of defined endosomal compartments. Cell-free avidin-biotin binding assays have also been used to study ligand segregation and sorting (Wessling-Resnick and Braell, 1990) and microtubule-dependent transport to late endosomes (Aniento et al., 1993); the results in general agree with conclusions from alternative fusion assays based on antibody-antigen interactions (Diaz et al., 1988; Colombo et al., 1992a,b).

What is the physical basis for the enhancement of BODIPY-avidin fluorescence in response to biotin binding? Johnson et al. (1991) and Karolin et al. (1994) have shown that the BODIPY fluorescence lifetime, quantum yield, and spectra did not change with pH and solvent polarity. Therefore, the enhancement of the BODIPY-avidin fluorescence is probably not due to a change in the polarity of the BODIPY environment after biotin binding. BODIPY fluorescence, however, is sensitive to the aromatic amino acids tyrosine and tryptophan (Karolin et al., 1994). By x-ray crystallography, avidin is a tetramer in which each monomer consists of an eight-stranded antiparallel β-barrel (Pugliese et al., 1993). The biotin binding site is located in a deep pocket near the center of the barrel in which two of the four tryptophan residues reside. The blue shift of the tryptophan fluorescence in avidin and BODIPY-avidin upon biotin binding suggests that a conformational change occurs in which the tryptophans move to a relatively shielded, nonpolar environment. Interestingly, the blue shift was accompanied by a decrease in the fluorescence of avidin and an increase in the fluorescence of BODIPY-avidin. These findings, taken together with the small change in BODIPY fluorescence lifetime upon biotin binding, suggest a static interaction between tryptophan and BODIPY chromophores in the absence of biotin, resulting in fluorescence quenching of both chromophores. Biotin binding to BODIPY-avidin results in a protein conformational change, which may weaken the interactions, and thus enhances both BODIPY and tryptophan fluorescence.

Previous studies of endosome fusion in vivo utilized the quenching of fluorescein conjugates (FITC-macroglobulin and FITC-transferrin) by antifluorescein antibodies (Salzman and Maxfield, 1988, 1989). Digital image processing was used to demonstrate intracellular fusion (Salzman and Maxfield, 1988) and to estimate half-times for the segregation and recycling of internalized makers (Salzman and Maxfield, 1989). The analysis was carried out on fixed cells utilizing a pseudo-ratio imaging approach based on the pH dependence of FITC quenching by the antifluorescein antibody. In contrast, the avidin-biotin fluorescence assay reported here can be used to visualize real-time fusion events in living cells by direct ratio imaging. Another advantage is that the large ratio of BODIPY-to-TMR signal ratios for fused versus unfused endosomes facilitates the detection of fusion events in individual endosomes with high sensitivity. In general agreement with the results of Maxfield and coworkers, our results demonstrate that internalized fluid-phase markers rapidly reach fusion-inaccessible compartments (Fig. 4); in BHK cells at 37°C, approximately half of

the avidin-labeled endosomes were accessible for fusion with biotin-albumin-labeled endosomes after a 5- to 10-min chase period. Remarkably, after a 10-min chase period, no avidin-labeled endosomes fused with biotin-transferrin-labeled endosomes, indicating the transport of the fluorescent avidin to a compartment that is inaccessible for fusion with early/recycling endosomes.

A Monte Carlo mathematical model was developed to interpret f_{fusion} values in terms of distinct cellular events, including heterogeneity in endosome maturation, transient endosome residence in an intermediate compartment, and endosome entry into a fusion-inaccessible compartment. Data fitting for the biotin-albumin pulse-chase experiments required the existence of an intermediate-fusion compartment; data fitting for the biotin-transferrin studies required the existence of a fusion-inaccessible compartment. Although the precise values of fitted model parameters probably have limited physical significance because of the simplicity of the model, we believe that the qualitative predictions of the model are valid. An alternative approach to describe endosomal trafficking involves kinetic modeling, in which rate parameters are introduced to describe endosome transit between distinct compartments (Ciechanover et al., 1983; Linderman and Lauffenburger, 1988; Ghosh and Maxfield, 1995). A Monte Carlo approach was utilized here because of the complexity of the pulse-chase protocols and to minimize the number of model assumptions and independent model parameters. Analysis of an extensive body of quantitative fusion data will be required to assess the ultimate utility of various modeling approaches for endosome transport.

Additional pulse-chase experiments were carried out to test a series of putative modulators of endosome fusion. Endosome fusion was remarkably inhibited by lowered temperature, the protein kinase inhibitor staurosporine, and the tyrosine kinase inhibitor genistein; lesser inhibition was found for the vacuolar proton pump inhibitor bafilomycin A1 and a phorbol ester, with no significant effect of a cAMP agonist. These inhibitor screening studies provided initial empirical information about in vivo effects on endosome fusion. It is emphasized here that definition of inhibitor sites of action and molecular mechanisms requires additional investigation by complementary approaches, which is beyond the scope of this study.

There are several significant technical concerns. As discussed previously (Zen et al., 1992), potential difficulties in the use of separate chromophores for ratio imaging microscopy are differential photobleaching and (when labeling stoichiometry is low) statistical heterogeneity in chromophore density. No photobleaching was detected with the specific chromophores, illumination intensities/times, and optical/detection hardware used here. Heterogeneity in chromophore density as manifested by differential trafficking was also probably a minor concern, based on the shape of the unimodal distribution of B/T ratios in Fig. 3 *B*. Another issue is the intrinsic variability in ratio determination for individual endosomes and from cell to cell. Because of the small endosome diameter and the limited number of chromophores per endosome, potential difficulties arise in the detection of weak signals from point-like particles, some of which appear as diffraction-limited Airy disks (Shi et al., 1991; Inoue, 1989). The detection system utilized a high magnification, high numerical aperture objective with a nearly 100% efficient, cooled CCD camera detector. The endosome identification/analysis software was optimized to detect endosomes with minimal selection bias and to determine area-integrated pixel intensities in a manner that was insensitive to the precise definition of endosome boundaries and background levels. Nevertheless, the precision of ratio values was limited by intrinsically low signal levels and inaccuracies in defining boundaries of complex-shaped endosomes and in subtraction of nonuniform background arising from out-of-focus fluorescence. The relatively large fluorescence enhancement of the BODIPY chromophore was important to detect fusion events in this challenging setting of low light levels and small labeled endosomes. Finally, we noted moderate cell-to-cell heterogeneity in distributions of endosome fluorescence ratio values, which may be related to different stages of the cell cycle. Therefore the interpretation of data required analysis of endosomes from multiple cell preparations.

Notwithstanding these technical caveats, the avidin-biotin fluorescence assay reported here permits spatially resolved measurement of the fusion of individual fluorescently labeled endosomes in living cells. A similar strategy utilizing BODIPY-labeled avidin should be applicable to real-time cell-free analysis of vesicular fusion kinetics, in which separate vesicle populations are labeled with appropriate avidin and biotin markers. In living cells, the fusion assay might also be used to quantify fusion between components of the endocytic and secretory pathways, utilizing a liposome-fusion approach developed recently to label the aqueous compartment of *trans*-Golgi in living cells (Seksek et al., 1995). Finally, the introduction of additional fluorescent labels on the avidin and biotin markers should allow for simultaneous measurement of vesicle fusion and pH or ion concentrations for definition of the determinants of vesicle fusion.

APPENDIX: Mathematical model of endosome fusion

A Monte Carlo computer model of endosome fusion was developed to predict the fraction of avidin-labeled endosomes that fuse with biotin-labeled endosomes in pulse-chase studies. The experimentally defined times for avidin pulse (T1), chase (C1), biotin pulse (T2), and final chase (C2) are first defined (Fig. 7). An avidin-labeled endosome is created at time *TA* determined as a uniformly distributed random number between times 0 and T1. Similarly, a biotin-labeled endosome is created at time *TB* between times T1 + C1 and T1 + C1 + T2. A large number of endosome pairs are generated by the Monte Carlo approach (Bicknese et al., 1992) in order to calculate the fraction of avidin-labeled endosomes that fuse with biotin-labeled endosomes by applying a series of logical constraints (Eqs. A1 to A3 below). The program (implemented in Basic 5.0, available on request) computes the fate of 10^4 endosomes in ~3 s using a 486 66 MHz

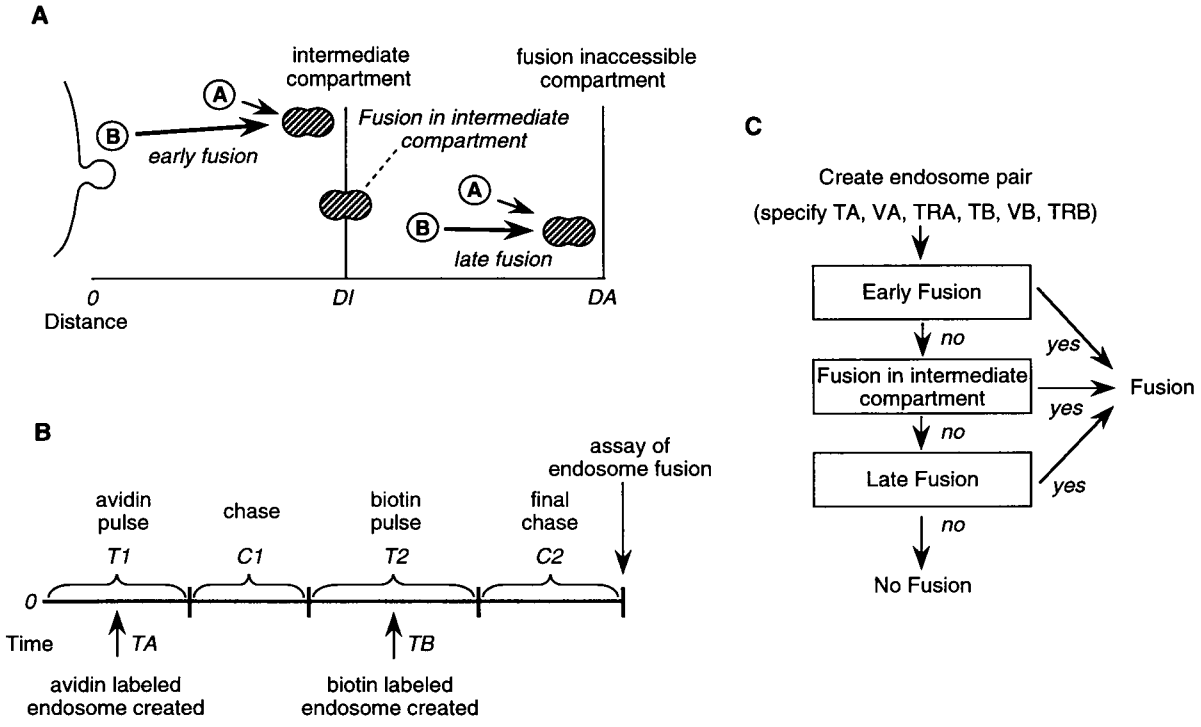

FIGURE 7 Mathematical model of in vivo endosome fusion. (*A*) Schematic of endocytosis showing Ⓐ avidin- and Ⓑ biotin-labeled endosomes, an intermediate compartment at *DI* and a fusion-inaccessible compartment at *DA*. Early fusion, fusion in the intermediate compartment, and late fusion are indicated. (*B*) Timeline for pulse-chase protocols showing avidin pulse, chase, biotin pulse, and final chase. Avidin- and biotin-labeled endosomes are created at random times *TA* and *TB* during their respective pulses. (*C*) Logic for computation of endosome fusion. See text and Appendix for details.

cpu; the fraction of fused endosomes generally changed by <0.001 when 10^5 endosome pairs were generated.

The model incorporates 1) heterogeneity in endosome properties, 2) fusion inaccessibility, and 3) an intermediate compartment. To introduce endosome heterogeneity, an average dimensionless velocity $V = 1$ for endosome transport was assigned; the velocity parameter can be thought of as an effective rate of endosome transit between compartments. Velocities of each avidin- (*VA*) and biotin-labeled (*VB*) endosome were calculated from *V* using computer-generated Gaussian-distributed random numbers with mean *V* and standard deviation *SV*. *SV* provides a quantitative index of endosome heterogeneity. Fusion inaccessibility occurs when an avidin-labeled endosome reaches distance *DA* before fusion occurs. An intermediate compartment or rest area is a compartment located at a distance *DI* in which endosomes reside for times *TRA* and *TRB* (for avidin- and biotin-labeled endosomes). *TRA* and *TRB* are computer-generated exponentially distributed random numbers with mean intermediate compartment residence time *TM*. Model parameters are thus *SV*, *DA*, *DI*, and *TM*. Vesicle heterogeneity, fusion inaccessibility, and/or the intermediate compartment can be eliminated from the model by setting *SV*, 1/*DA*, and/or *TM* equal to zero.

The logic of the model is shown in Fig. 7. An endosome pair is created by specification of *TA*, *VA*, *TRA*, *TB*, *VB*, and *TRB* on the basis of pulse-chase times and model parameters. The pair produces a fusion event if the avidin- and biotin-labeled endosomes meet proximal to the intermediate compartment (early fusion), in the intermediate compartment, or distal to the intermediate compartment but proximal to inaccessibility distance *DA* (late fusion). Early fusion occurs if the biotin-labeled endosome catches up with the avidin-labeled endosome before reaching *DI* and before total time (T = T1 + C1 + T2 + C2) expires,

$$(TA - TB) \cdot VB \cdot VA/(VA - VB) < DI \qquad \text{(A1)}$$

$$\text{and} \quad (VA \cdot TA - VB \cdot TB)/(VA - VB) < T$$

If early fusion does not occur, fusion in the intermediate compartment occurs if the avidin-labeled endosome leaves the compartment after the biotin-labeled endosome enters the compartment, provided the biotin-labeled endosome enters the compartment before *T*,

$$TA + TRA + DI/VA > TB + DI/VB \quad \text{and}$$

$$TB + DI/VB < T \qquad \text{(A2)}$$

If early and intermediate compartment fusion do not occur, late fusion occurs if the biotin-labeled endosome catches up with the avidin-labeled endosome before reaching *DA* and before *T*,

$$(TA + TRA - TB - TRB) \cdot VB \cdot VA/(VA - VB) < DA \quad \text{and} \qquad \text{(A3)}$$

$$[(TA + TRA) \cdot VA - (TB + TRB) \cdot VB]/(VA - VB) < T$$

These conditions are applied to each endosome pair to compute the fraction of avidin-label edendosomes that show a fusion signal.

We thank Dr. Steve Bicknese for assistance in fluorescence lifetime measurements and computer modeling, and Drs. H. Pin Kao and N. Periasamy for modification of the image analysis software. This work was supported by grants HL42368 and DK43840 from the National Institutes of Health, RDP grant R613 from the National Cystic Fibrosis Foundation, and a grant from the California Tobacco-Related Disease Program. Dr. Emans was supported by a fellowship from the Boehringer Ingelheim Fonds and a short-term fellowship (SF 250–93) from the International Human Frontiers Science Program.

REFERENCES

Aniento, F., N. Emans, G. Griffiths, and J. Gruenberg. 1993. Cytoplasmic dynein-dependent vesicular transport from early to late endosomes. *J. Cell Biol.* 123:1373–1387.

Bicknese, S., Z. Shahrohk, S. B. Shohet, and A. S. Verkman. 1992. Single photon radioluminescence. I. Theory and spectroscopic properties. *Biophys. J.* 63:1256–1266.

Bradbury, N., and R. J. Bridges. 1992. Endocytosis is regulated by protein kinase A, but not protein kinase C in a secretory epithelial cell line. *Biochem. Biophys. Res. Commun.* 184:1173–1180.

Braell, W. A. 1992. Detection of endocytic vesicle fusion in vitro, using assay based on avidin-biotin association reaction. *Methods Enzymol.* 219:12–20.

Ciechanover, A., A. L. Schwartz, A. Dautry-Varsat, and H. F. Lodish. 1983. Kinetics of internalization and recycling of transferrin and the transferrin receptor in a human hepatoma cell line. Effect of lysosomotropic agents. *J. Biol. Chem.* 258:9681–9689.

Clague, M. J., S. Urbe, F. Aniento, and J. Gruenberg. 1994. Vacuolar ATPase activity is required for endosomal carrier vesicle formation. *J. Biol. Chem.* 269:21–24.

Colombo, M. I., J. M. Lenhard, L. S. Mayorga, and P. D. Stahl. 1992a. Reconstitution of endosome fusion: identification of factors necessary for fusion competency. *Methods Enzymol.* 219:32–44.

Colombo, M. I., L. S. Mayorga, P. J. Casey, and P. D. Stahl. 1992b. Evidence of a role for heterotrimeric GTP-binding proteins in endosome fusion. *Science.* 255:1695–1697.

Constantinescu, S. N., C. D. Cernescu, and L. M. Popescu. 1991. Effects of protein kinase C inhibitors on viral entry and infectivity. *FEBS Lett.* 292:31–33.

Diaz, R., L. Mayorga, and P. Stahl. 1988. In vitro fusion of endosomes following receptor-mediated endocytosis. *J. Biol. Chem.* 263: 6093–6100.

Fallon, R. J., and M. Danaher. 1992. The effect of staurosporine, a protein kinase inhibitor, on asialoglycoprotein receptor endocytosis. *Exp. Cell Res.* 203:420–426.

Fallon, R. J., M. Danaher, R. L. Saylors, and A. Saxena. 1994. Defective asialoglycoprotein receptor endocytosis mediated by tyrosine kinase inhibitors. Requirement for a tyrosine in the receptor internalization signal. *J. Biol. Chem.* 269:11011–11017.

Ghosh, R. N., and F. R. Maxfield. 1995. Evidence for nonvectorial, retrograde transferrin trafficking in early endosomes of HEp2 cells. *J. Cell Biol.* 128:549–561.

Goda, Y., and S. R. Pfeffer. 1988. Selective recycling of the mannose-6-phosphate/IGF-11 receptor to the trans Golgi network in vitro. *Cell.* 55:309–320.

Goda, Y., and S. R. Pfeffer. 1989. Cell-free systems to study vesicular transport along the secretory and endocytic pathways. *FASEB J.* 3:2488–2495.

Goda, Y., and S. R. Pfeffer. 1991. Identification of a novel, N-ethylmaleimide-sensitive cytosolic factor required for vesicular transport from endosomes to the trans-Golgi network in vitro. *J. Cell Biol.* 112:823–831.

Goldstein, J. L., M. S. Brown, R. G. W. Anderson, D. W. Russell, and W. J. Schneider. 1985. Receptor mediated endocytosis: concepts emerging from the LDL receptor system. *Annu. Rev. Cell Biol.* 1:1–39.

Gorvel, J.-P., P. Chavrier, M. Zeriel, and J. Gruenberg. 1991. rab5 controls early endosome fusion in vitro. *Cell.* 64:915–925.

Green, N. M. 1963. Avidin. 1. The use of 14C-biotin for kinetic studies and for assay. *Biochem. J.* 89:585–591.

Green, N. M. 1975. Avidin. *Adv. Protein Chem.* 29:85–133.

Gruenberg, J. E., and K. E. Howell. 1989. Membrane traffic in endocytosis: insights from cell-free assays. *Annu. Rev. Cell Biol.* 5:453–481.

Gruenberg, J. E., G. Griffiths, and K. E. Howell. 1989. Characterization of the early endosome and putative endocytic carrier vesicles in vivo and with an assay of vesicle fusion in vitro. *J. Cell Biol.* 108:1301–1316.

Gruenberg, J. E., and J.-P. Gorvel. 1992. In vitro reconstitution of endocytic vesicle function. *In* Protein Targeting: A Practical Approach. A. L. Magee and T. Wileman, editors. Oxford University Press, New York. 187–215.

Inuoe, S. 1989. Imaging of unresolved objects, superresolution and precision of distance measurement, with video microscopy. *In* Methods in Cell Biology, Vol. 30. D. L. Taylor and Y.-L. Wang, editors. 85–112.

Johnson, I. D., H. C. Kang, and R. P. Haugland. 1991. Fluorescent membrane probes incorporating dipyrromethene boron difluoride fluorophores. *Anal. Biochem.* 198:228–237.

Karolin, J., L. B. A. Johansson, L. Standberg, and T. Ny. 1994. Fluorescence and absorption spectroscopic properties of dipyrromethene boron difluoride (BODIPY) derivatives in liquids, lipid membranes, and proteins. *J. Am. Chem. Soc.* 116:7801–7806.

Kornfeld, S., and I. Mellman. 1989. The biogenesis of lysosomes. *Annu. Rev. Cell Biol.* 5:483–525.

Kurzban, G. P., G. Gitlin, E. A. Bayer, M. Wilchek, and P. M. Horowitz. 1989. Shielding of tryptophan residues of avidin by the binding of biotin. *Biochemistry.* 28:8537–8542.

Linderman, J. J., and D. A. Lauffenburger. 1988. Analysis of intracellular receptor/ligand sorting in endosomes. *J. Theor. Biol.* 132:203–245.

Luton, F., M. Buferne, J. Davoust, A. M. Schmitt-Verhulst, and C. Boyer. 1994. Evidence for protein tyrosine kinase involvement in ligand-induced TCR/CD3 internalization and surface redistribution. *J. Immunol.* 153:63–72.

Palokangas, H., K. Metsikko, and K. Vaananen. 1994. Active vacuolar H+ATPase is required for both endocytic and exocytic processes during viral infection of BHK-21 cells. *J. Biol. Chem.* 269:17577–17585.

Przyjazny, A., N. G. Hentz, and L. G. Bachas. 1993. Sensitive and selective liquid chromatographic postcolumn reaction detection system for biotin and biocytin using a homogeneous fluorophore-linked assay. *J. Chromatogr.* 654:79–86.

Pugliese, L., A. Coda, M. Malcovati, and M. Bolognesi. 1993. Three-dimensional structure of the tetragonal crystal form of egg-white avidin in its functional complex with biotin at 2.7 A resolution. *J. Mol. Biol.* 231:698–710.

Pure, E., and L. Tardelli. 1992. Tyrosine phosphorylation is required for ligand-induced internalization of the antigen receptor on B lymphocytes. *Proc. Natl. Acad. Sci. U.S.A.* 89:114–117.

Reaves, B., and G. Banting. 1994. Vacuolar ATPase inactivation blocks recycling to the trans-Golgi network from the plasma membrane. *FEBS Lett.* 345:61–66.

Salzman, N. H., and F. R. Maxfield. 1988. Intracellular fusion of sequentially formed endocytic compartments. *J. Cell Biol.* 106:1083–1091.

Salzman, N. H., and F. R. Maxfield. 1989. Fusion accessibility of endocytic compartments along the recycling and lysosomal endocytic pathways in intact cells. *J. Cell Biol.* 109:2097–2104.

Seksek, O., J. Biwersi, and A. S. Verkman 1995. Direct measurement of *trans*-Golgi pH in living cells and regulation by second messengers. *J. Biol. Chem.* 270:4967–4970.

Shi, L.-B., K. Fushimi, H.-R. Bae, and A. S. Verkman 1991. Heterogeneity in acidification measured in individual endocytic vesicles isolated from kidney proximal tubule. *Biophys. J.* 59:1208–1217.

Thevenin, B. J. M., N. Periasamy, S. B. Shohet, and A. S. Verkman. 1994. Segmental dynamics of the cytoplasmic domain of erythrocyte band 3 determined by time-resolved fluorescence anisotropy: sensitivity to pH and ligand binding. *Proc. Natl. Acad. Sci. U.S.A.* 91:1741–1745.

Van Hoek, A. N., and A. S. Verkman 1992. Functional reconstitution of the isolated erythrocyte water channel CHIP28. *J. Biol. Chem.* 267: 18267–18269.

Wessling-Resnick, M., and W. A. Braell. 1990. The sorting and segregation mechanism of the endocytic pathway is functional in a cell-free system. *J. Biol. Chem.* 265:690–699.

Woodman, P. G., D. I. Mundy, P. Cohen, and G. Warren. 1992. Cell-free fusion of endocytic vesicles is regulated by phosphorylation. *J. Cell Biol.* 116:331–338.

Zen, K., J. Biwersi, N. Periasamy, and A. S. Verkman 1992. Second messengers regulate endosomal acidification in Swiss 3T3 fibroblasts. *J. Cell Biol.* 119:99–110.